2023 CCM & IMEKO International Conference on Pressure and Vacuum Metrology
IMEKO TC-16 2023
Washington DC, USA, May 15-19, 2023

Working equation for a Fabry-Perot cavity based optical pressure standard

Yuanchao Yang[1], Patrick F. Egan[2], Tom Rubin[3]

[1] *National Institute of Metrology, Beijing 10029, China, yangyc@nim.ac.cn*
[2] *National Institute of Standards and Technology, Gaithersburg, MD 20899, USA, egan@nist.gov*
[3] *Physikalisch-Technische Bundesanstalt, Berlin, 10587, Germany, tom.rubin@ptb.de*

***Abstract* – From basics of Fabry-Perot (FP) resonator and roundtrip phase, a complete working equation for a FP cavity based optical pressure standard (OPS) is derived and presented which includes corrections of reflection phase-shift, diffraction and pressure-induced distortion. The correction from diffraction, i.e. Gouy phase, is negligible. To operate an OPS as a primary standard, two unknown parameters, i.e. mirror dispersion coefficient ϵ_α and pressure distortion coefficient d_m, in the working equation should be determined independently. Methods to determine ϵ_α and d_m are described and applied to an OPS developed at the National Institute of Metrology (NIM), China. Thermodynamic effect observed in the determination of d_m is also discussed.**

I. INTRODUCTION

A Fabry-Perot (FP) cavity based optical pressure standard (OPS) is very promising to be the next generation primary standard covering the range from 1 Pa to 1 MPa, due to its high accuracy and universality [1-7]. To operate an OPS at the highest level of accuracy, a consensus should be achieved on its working equation, which converts the measurand of frequency and temperature to the pressure. The resonance condition in a FP cavity can be described by the concept of roundtrip phase and integer half-wavelengths. The accurate description should take into account the physics at the mirror reflection, which can be described using the reflection phase-shift or penetration depth. However, use of a penetration depth in FP frequency metrology is a tricky undertaking [8, 9]. This article presents a complete working equation for an OPS derived from the basics of FP resonator and roundtrip phase, which includes corrections of reflection phase-shift and Gouy phase, i.e. the effect of diffraction in Gaussian optics. In addition, the working equation accounts for pressure-induced distortion, which is the major correction. For the reflection phase-shift, two types of dielectric-stack mirrors are considered, i.e. the so-called type-H and type-L. The dependence of reflection phase-shift on frequency causes an error when the resonant frequency changes. Hence this effect is also called as mirror dispersion. The diffraction effect is expressed by adding a Gouy phase component to the roundtrip phase. The Gouy phase is affected by the refractive index of gas on the path of laser beam, hence it causes an error if it is neglected.

To operate an OPS as a primary standard, all unknown parameters in the working equation should be determined independently, i.e. without reference to other pressure standard. Methods to determine the mirror dispersion coefficient and pressure distortion coefficient are described in this article. The application of the methods to an OPS developed at the National Institute of Metrology (NIM) [4] is also presented.

II. WORKING EQUATION

Resonance condition for a two-mirror FP cavity which accounts for the reflection phase-shift ϕ_R and the Gouy phase ϕ_G due to diffraction is:

$$2\pi m = \frac{4\pi L}{c} n\nu + 2\phi_\mathrm{R} - 2\phi_\mathrm{G} \ . \qquad (1)$$

Here, m is the integer mode number, L is the separation between the front faces of the mirrors, c is the speed of light in vacuum, n is the refractive index of the medium between the mirrors and ν is the optical frequency.

ϕ_R is dependent on the frequency ν by a coefficient α, and is expressed as:

$$\phi_\mathrm{R} = \phi_0 + \alpha(\nu - \nu_\mathrm{des}) \ . \qquad (2)$$

The fundamental requirement that ϕ_R is signed such that it adds to roundtrip phase is emphasized (refection occurs inside the mirror stack). Here, ϕ_0 is the phase-shift at the design frequency ν_des of the mirrors, and equals π or 0 depending on whether a high- or low-index layer, respectively, faces the incident laser. As one operates away from ν_des, the $\phi_\mathrm{R}(\nu)$ dependence is captured by $\alpha = d\phi/d\nu$. The mirror phase response α is customarily specified with vacuum as the incident medium, but it depends on refractive index of the medium in front of the dielectric stacks [8, 9]. A type-H quarterwave stack mirror has the high-index layer facing the incident laser, and $\alpha_\mathrm{gas} = n\alpha$. A type-L mirror has the low-index layer facing the incident laser, and $\alpha_\mathrm{gas} = \frac{1}{n}\alpha \approx (2-n)\alpha$ when $n - 1 \ll 1$. The type-H and type-L mirrors are schematically illustrated in Fig. 1.

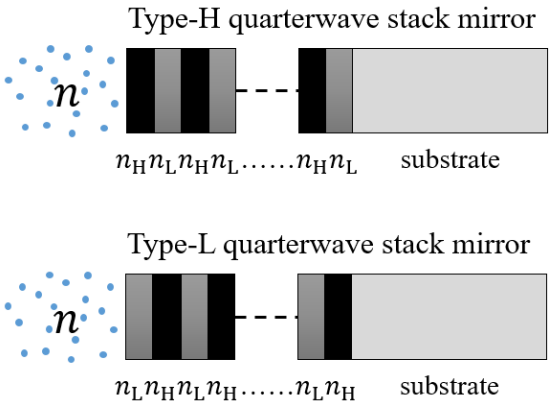

Fig. 1. Schematic drawings of the type-H and type-L mirrors.

It is pointed out that ϕ_0 is independent of gas in front of the stack. Fresnel equations govern that any pair of reflecting surfaces with complex reflection coefficients r_1 (a real number here) and $r_2 e^{i\theta}$ can be treated as a single equivalent reflecting surface at the location of the first reflection. The reflecting pair have an equivalent reflection coefficient

$$r_{\mathrm{eq}} = \frac{-r_1 + e^{i\varphi} r_2 e^{i\theta}}{1 - e^{i\varphi} r_1 r_2 e^{i\theta}} \ . \qquad (3)$$

As written, the formula assumes no losses, and φ is the roundtrip phase-shift of light passing through the first dielectric layer. The amplitude reflection coefficient at the first surface is given by the usual Fresnel formula $r_1 = (n - n_1)/(n + n_1)$, where n is the refractive index of the gas and n_1 is the refractive index of the first di-electric layer. The amplitude coefficient r_1 will change as gas is admitted (because n changes), but it is always a real number if a lossless media is assumed with real refractive indices. If $\varphi + \theta$ is 0 or a multiple of π, the expression for r_{eq} is real. Note that the only value in equation (3) that changes when gas is added is r_1. Consequently, r_{eq} remains real even though r_1 changes, and in this case the phase-shift does not change when gas is added; it is entirely independent of changes in the first surface reflection. Alternatively stated, at the design frequency, ϕ_{R} is exactly 0 or π-multiple, and has no dependence on gas in front of the mirror. As one moves away from the design frequency, deviations from ϕ_0 are indeed denpendent on n, and this is accounted for via $\alpha_{\mathrm{gas}} = n\alpha$ or $\alpha_{\mathrm{gas}} = (2 - n)\alpha$, for the case of type-H and type-L mirrors, respectively.

The Gouy phase-shift of a Gaussian beam changes as a function of refractive index, which is $\arctan\left[z\lambda_{\mathrm{vac}}/(\pi n w_0^2)\right]$, with λ_{vac} the vacuum-wavelength, w_0 the beam waist, and z the propagation distance in a medium of refractive index n [10]. In Gaussian optics, the Rayleigh range is defined as $z_{\mathrm{R}} = \frac{\pi n w_0^2}{\lambda_{\mathrm{vac}}}$. Clearly, the Gouy phase-shift depends on refractive index, which at first-order looks like $\phi_{\mathrm{G\_gas}} \approx \frac{1}{n}\phi_{\mathrm{G\_vac}}$. An approximate derivation for a FP cavity refractometer could proceed with $\phi_{\mathrm{G\_gas}} \approx (2 - n)\phi_{\mathrm{G\_vac}}$, but it relies on small angles and $L \ll R$. For some cavities in which $\frac{L}{R} \to 1$, the approximation would produce estimates of the Gouy phase effect incorrect by a factor of 4. The estimate can be refined as follows.

When the input laser is mode-matched to a plano-concave FP cavity of length L, the cavity mode has $R = L + \frac{z_{\mathrm{R}}^2}{L}$, so $z_{\mathrm{R}} = \sqrt{(R - L)L}$. From the definition of Rayleigh range above, z_{R} is proportional to refractive index, so $z_{\mathrm{R\_gas}} = n z_{\mathrm{R}}$. Recall the Gouy phase $\phi(z) = \tan^{-1}\left(\frac{z}{z_{\mathrm{R}}}\right)$, so when mode-matched in vacuum $\phi_{\mathrm{G\_vac}} = \tan^{-1}\left(\sqrt{\frac{L}{R-L}}\right)$, and in gas $\phi_{\mathrm{G\_gas}} = \tan^{-1}\left(\frac{1}{n}\sqrt{\frac{L}{R-L}}\right)$. The Taylor expansion for $\tan^{-1}\left(\frac{1}{n}\sqrt{\frac{L}{R-L}}\right)$ about the nominal phase $\sqrt{\frac{L}{R-L}}$ is

$$\tan^{-1}\left(\frac{1}{n}\sqrt{\frac{L}{R-L}}\right) = \tan^{-1}\left(\sqrt{\frac{L}{R-L}}\right) + \frac{\frac{1}{n}\sqrt{\frac{L}{R-L}}\sqrt{\frac{L}{R-L}}}{1+\frac{L}{R-L}} + \cdots \ ,$$

so the difference in Gouy phase between gas and vacuum conditions is

$$\phi_{\mathrm{G\_gas}} - \phi_{\mathrm{G\_vac}} = \frac{\sqrt{\frac{L}{R-L}}\left(\frac{1}{n}-1\right)}{1+\frac{L}{R-L}} \ ,$$

and using $\frac{1}{n} \approx 2 - n$, $\phi_{\mathrm{G\_gas}} = \phi_{\mathrm{G\_vac}} - (n-1)\frac{z_{\mathrm{R}}}{R}$.

From the basic statement of equation (1), the resonance frequency at vacuum can be written as

$$\nu_{\mathrm{vac}} = \frac{c}{2L + \alpha c/\pi}\left(m - \frac{\phi_0 - \alpha\nu_{\mathrm{des}}}{\pi} + \frac{\phi_{\mathrm{G\_vac}}}{\pi}\right) \ , \qquad (4)$$

and with gas inside the cavity (ignoring the compression of L here)

$$\nu_{\mathrm{gas}} = \frac{c}{2nL + \alpha_{\mathrm{gas}} c/\pi}\left(m + \Delta m - \frac{\phi_0 - \alpha_{\mathrm{gas}}\nu_{\mathrm{des}}}{\pi} + \frac{\phi_{\mathrm{G\_gas}}}{\pi}\right) \ . \qquad (5)$$

With the parameter $\epsilon_\alpha = \frac{\alpha c}{2\pi L}$, subtracting equation (5) from equation (4) and solving for refractivity yields, for the type-H mirror:

$$n - 1 = \frac{(\nu_{\mathrm{vac}} - \nu_{\mathrm{gas}})(1 + \epsilon_\alpha) + \Delta m\frac{c}{2L}}{\nu_{\mathrm{gas}} + \epsilon_\alpha(\nu_{\mathrm{gas}} - \nu_{\mathrm{des}}) + \frac{c}{2\pi L}\sqrt{\frac{L}{R}}} \ , \qquad (6)$$

and for the type-L mirror:

$$n - 1 = \frac{(\nu_{\mathrm{vac}} - \nu_{\mathrm{gas}})(1 + \epsilon_\alpha) + \Delta m\frac{c}{2L}}{\nu_{\mathrm{gas}} - \epsilon_\alpha(\nu_{\mathrm{gas}} - \nu_{\mathrm{des}}) + \frac{c}{2\pi L}\sqrt{\frac{L}{R}}} \ . \qquad (7)$$

E.g., for $L = 10$ cm, $R = 50$ cm, $\epsilon_\alpha \approx 7.5 \times 10^{-6}$, $(\nu_{\mathrm{gas}} - \nu_{\mathrm{des}}) < 10$ THz and $\nu_{\mathrm{gas}} = 474$ THz (633 nm

wavelength), neglecting the second and third terms in the denominator would cause errors < 0.2 parts per million (ppm) and < 0.5 ppm, respectively. For targeting pressure uncertainty of 10 ppm (k=2), these two terms can be ignored, and equation (6) and (7) are essentially the same no matter what type of the dielectric-stack mirror is. Furthermore, the generalization of equation (6) and (7) is enabled by ϵ_α, the so-called mirror dispersion coefficient, which is proportional to α and reversely proportional to the cavity length L. Hence the mirror dispersion is an end-effect. For a cavity length of 100 mm, this correction for $n-1$, then pressure, is at the level of 10 ppm. The phase response α must be determined for any specific dielectric stack. For quarterwave stacks in general, α is about three times larger for a type-L mirror compared to a type-H mirror.

Considering the compression of L induced by a pressure p, the left term of equation (6) and (7) turns to be $n-1-nd_mp$, with d_m as the distortion coefficient of the cavity. Finally, the equation below applies.

$$n-1-nd_mp=\frac{(\nu_{\mathrm{vac}}-\nu_{\mathrm{gas}})(1+\epsilon_\alpha)+\Delta m\frac{c}{2L}}{\nu_{\mathrm{gas}}} \quad . \qquad (8)$$

Equation (8) is the final expression. To use it, one must determine L using an absolute resonance frequency, together with knowledge of reflection and Gouy phase-shifts. Alternatively, $\frac{c}{2L}$ is related to the free spectral range (FSR=ν_{fsr}), which can be measured conveniently. From equation (4), we have $\nu_{\mathrm{fsr}}=\frac{c}{2L+\alpha c/\pi}=\frac{c}{2L(1+\epsilon_\alpha)}$. Hence, equation (8) can be written as:

$$n-1-nd_mp=\frac{\nu_{\mathrm{vac}}-\nu_{\mathrm{gas}}+\Delta m\nu_{\mathrm{fsr}}}{\nu_{\mathrm{gas}}}(1+\epsilon_\alpha) \quad . \qquad (9)$$

Based on equation (9), the Lorentz-Lorenz equation and the equation of state, the working equation to calculate pressure can be obtained, as has been used in Ref. [3] and [4].

III. EXPERIMENTAL DETERMINATION OF ϵ_α AND d_m

There are two unknown parameters in equation (9), i.e. the mirror dispersion coefficient ϵ_α and pressure distortion coefficient d_m, which should be determined independently to make the OPS working as a primary pressure standard.

A. Mirror dispersion coefficient ϵ_α

The ϵ_α can be calculated using the mirror coating information provided by the manufacturer. Moreover, it can be validated, and its accuracy improved by in-situ measurements of ν_{fsr} and absolute resonance frequency of the cavity [11]. The approach is to deduce a mode number of resonance with accuracy of ~ 0.1. The fraction in the mode number is a result of the reflection phase-shift and Gouy phase. Equation (4) is equivalent to:

$$\nu_{\mathrm{vac}}=\nu_{\mathrm{fsr}}\left(m-\frac{\phi_0-\alpha\nu_{\mathrm{des}}}{\pi}+\frac{\phi_{\mathrm{G\_vac}}}{\pi}\right) \quad . \qquad (10)$$

Obviously, the ratio $\nu_{\mathrm{vac}}/\nu_{\mathrm{fsr}}$ is not an integer but with a decimal equal to $\frac{\alpha\nu_{\mathrm{des}}}{\pi}+\frac{\phi_{\mathrm{G\_vac}}}{\pi}$.

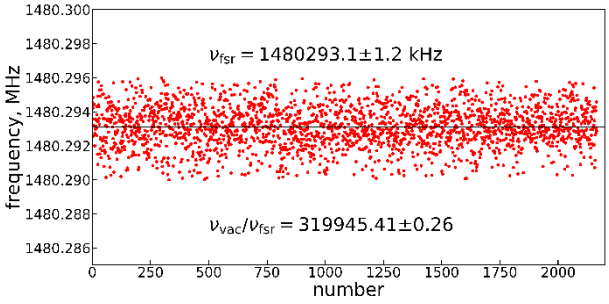

Fig. 2. Results of FSR measurements for the measurement cavity of the NIM OPS.

For the NIM OPS [4], the FSR of the measurement cavity was measured at vacuum by locking the laser frequency to two adjacent modes back and forth repeatedly, and the difference of its beat to the reference cavity was logged. The measurements were fully automated. Over 2000 data points were recorded as shown in Fig. 2. Taking the average and the statistic standard deviation of the data, ν_{fsr} was determined to be 1480293.1±1.2 kHz. The absolute frequency of one of the mode ν_{vac} was measured by linking it to an iodine stabilized helium-neon laser. Then the ratio $\nu_{\mathrm{vac}}/\nu_{\mathrm{fsr}}$ is calculated to be 319945.41±0.26. With the measured ratio, we have:

$$\frac{\alpha\nu_{\mathrm{des}}}{\pi}+\frac{\phi_{\mathrm{G\_vac}}}{\pi}=k+0.41\pm0.26 \quad . \qquad (11)$$

where k is an unknown integer. The Gouy phase is calculated to be $\phi_{\mathrm{G\_vac}}=\arcsin\left(\sqrt{L/R}\right)=0.46$, with $L=10$ cm and $R=50$ cm. It can be also determined by in-situ measurements using the astigmatic method [12], which is to slightly misalign the laser beam in order to excite transverse modes of higher order. With $\nu_{\mathrm{des}}=474$ THz, we obtained:

$$\alpha=0.663\times(k+0.26\pm0.26)\times10^{-14}\ \mathrm{rad/Hz} \quad . \qquad (12)$$

The manufacturer provided a value of 1.3129×10^{-14} rad/Hz without uncertainty information. Hence, k is most probably to be 2. Based on this, $\alpha=(1.50\pm0.17)\times10^{-14}$ rad/Hz, and $\epsilon_\alpha=(7.1\pm0.8)\times10^{-6}$.

B. Pressure distortion coefficient d_m

The pressure distortion coefficient d_m can be determined by the so-called two-gas method [13]. It is to compare the pressure measurements at a same pressure usually generated by a piston gauge (PG), with two gases of very different and known refractive indices,

respectively. Comparisons with PG measurements were done using nitrogen and helium at 80 kPa.

A preliminary d_m value was obtained by calibrating the OPS against a PG [4]. The preliminary d_m used in this article is 9.892×10^{-12} Pa^{-1}, which was adjusted from the value in Ref. [4] with the updated ϵ_α determined in this work. With this d_m value, the pressure differences of PG to OPS were plotted versus time. Figure 3 and 6 show the plots for nitrogen and helium, respectively.

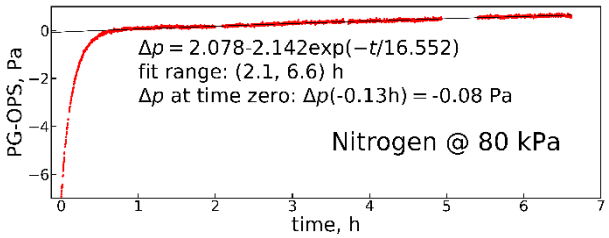

Fig. 3. Comparison of pressure between PG and OPS with preliminary d_m value using nitrogen at 80 kPa.

A fast rising can be seen in Fig. 3 at the beginning time. This indicates a thermodynamic process, during which the temperature of gas in the cavity mode was lower than the temperature measured by the standard platinum resistance thermometers (SPRT) located at the copper chamber housing the FP cavity, and the gas was heated up. The colder cavity at beginning was due to the heat-island effect and leak of heat. Before filling gas for pressure measurements, the copper chamber was turbo-pumped for over 12 h to minimize the outgassing effect. The FP cavity lost thermal connection to the copper chamber, and became colder because of heat leak.

The cavity was estimated to be ~ 58 mK colder than the copper chamber just before the gas filling. The estimation was based on the cavity baseline shift observed. With this initial condition, finite element analysis (FEA) was used to simulate the thermodynamic process after the gas filling.

Figure 4 shows the temperature contour of the copper chamber and the FP cavity at the time of 600 s after nitrogen filling. The maximum temperature gradient is ~ 35 mK. The time of 600 s is the typical starting time for pressure comparison measurements. The temperature difference between the gas in the mode and the SPRT causes pressure errors of the OPS. Figure 5 shows the difference of temperature between the mode and SPRT over 6 h. After 2 h, the difference is within 0.5 mK, corresponding to pressure error less than 1.6 ppm.

As shown in Fig. 3, the pressure difference went to a process of slow drift after 1 h. The drift was mainly attributed to the outgassing of water vapor [14]. The intrinsic pressure difference between the PG and OPS is deduced by fitting the slow drift part with an exponential decay function and extrapolating to the starting time of gas filling. To minimize the influence of temperature gradient, the data for fitting was selected after 2.1 h. The fitting results were shown in Fig. 3. The disagreement between the OPS and PG is only 0.08 Pa at nitrogen pressure of 80 kPa, i.e. 1 ppm. This result was expected, since the preliminary d_m value used was calibrated by the PG using nitrogen.

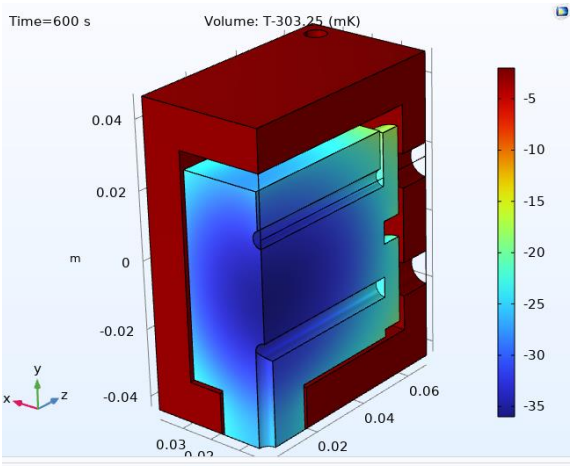

Fig. 4. Temperature contour of the copper chamber and the FP cavity at 600 s after filling of nitrogen.

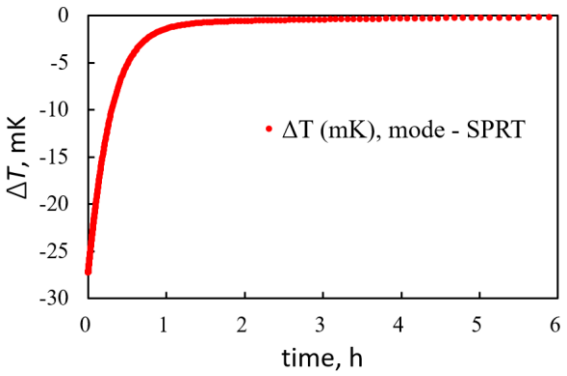

Fig. 5. Temperature difference between the gas in the cavity mode and the SPRT versus time.

The same measurement procedure was applied for helium, and the results were shown in Fig. 6. The trend shown in Fig. 6 is dominated by the helium diffusion into the cavity (ULE glass) [15, 16] and the outgassing, and the drift is much more remarkable than in the case of nitrogen. The thermodynamic process was not observed because its effect was minor compared to the drift, also the much higher thermal conductivity of helium than nitrogen shortened the thermo-equilibrium time.

The fitting results showed a disagreement of 34.84 Pa, i.e. 436 ppm at 80 kPa, between the OPS and PG. We can adjust the d_m value until the disagreements for nitrogen and helium are identical. This is the way to determine d_m without reference to the PG pressure. However, if we trust the helium result, the OPS would differ to the PG by 54 ppm. This is unlikely since the PG is a primary pressure standard at NIM and has obtained an equivalence of ~ 10 ppm in the international comparison of CCM.P-K6 [17]. At this stage, the purity of the helium needs to be checked

further, before utilizing the so-called two-gas method to determine d_m.

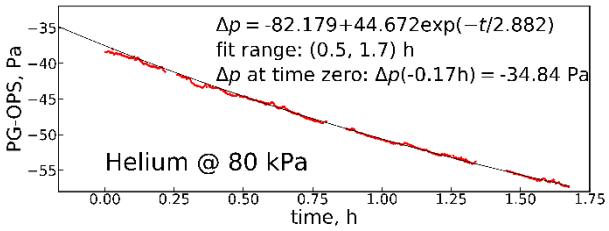

Fig. 6. Comparison of pressure between PG and OPS with preliminary d_m value using helium at 80 kPa.

IV. SUMMARY AND DISCUSSIONS

This article presented a derivation of equation for a FP refractometer with the consideration of reflection phase-shift, Gouy phase and pressure-induced distortion. The equation is a basis of the working equation for the OPS, as has been used in Ref. [3] and [4]. Approaches to experimentally determine two parameters in the working equation, ϵ_α and d_m, are introduced and applied to the NIM OPS. The working equation and the methods to determine ϵ_α and d_m are the basis to operate the OPS as a primary pressure standard.

The ultimate accuracy of an OPS is dependent on how well the dynamic polarizability of a second kind of gas except helium at the given optical frequency is determined. At present, the best achieved uncertainties by optical measurements are 7.3 ppm (k=2) for nitrogen [3] and 16 ppm (k=1) for argon [18]. Recently, the polarizability of argon was reported with accuracy of ~ 10 ppm (k=1), which was based on measurement of static polarizability scaled in frequency with dispersion coefficients from theoretical calculations [19]. Further reducing the uncertainties is the subject of current research. Nevertheless, if same reference values of polarizabilities are used, the consistency of OPSs built in different labs should agree within the ability to assess and/or control the gas temperature. From this point of view, OPSs are expected to outperform established standards. To validate this, an international comparison of the OPS at the highest level of accuracy is needed.

V. ACKNOWLEDGEMENTS

Yuanchao Yang acknowledges the funding from the National Institute of Metrology (Grant no. AKYZD2303-2). Tom Rubin acknowledges the funding via the 22 IEM MQB-Pascal project, which received funding from the European Partnership on Metrology, co-financed from the European Union's Horizon Europe Research and Innovation Programme and by the Participating States (Funder ID: 10.13039/100019599).

VI. APPENDIX: OPTIMIZED THERMAL DESIGN

Figure 5 discussed a key problem in an optical pressure standard: the temperature of the gas T interacting with the interferometer mode (the laser beam) must be known in the realization $p = \frac{2R}{3A_R}(n-1)T + \cdots$, with R the gas constant and A_R the molar polarizability of the gas. Traditional "contact thermometry" employs a resistance thermometer to sense the temperature of a body. In the case of Fig. 4, the resistance thermometer is embedded in the copper chamber, and is therefore separate in space from the laser beam. This setup risks undetected gradients, and inevitably leads to a settling-time needed before an optical pressure can be sampled after a gas fill. The settling-time is how long it takes the temperature gradient between the resistance thermometer and laser beam to approach zero. In general, short settling-times are preferred, because they allow fast measurement of pressure. As a desirability guideline for "fast", a traditional piston-gage will generate a known pressure within a few minutes of a gas fill.

Here is briefly mentioned a meta-analysis for settling-times of several extant optical pressure standards. The comparison is shown graphically in Fig 7. Evidently, the system discussed in the main text (Ref. [4]) takes about 6,000 s for the gradient between the resistance thermometer T_{sprt} and the interferometer mode T_{mode} to approach 0.1 mK. An error of 0.1 mK in the estimated temperature of the interferometer mode corresponds to an error of 0.3 μPa/Pa in an optical pressure standard.

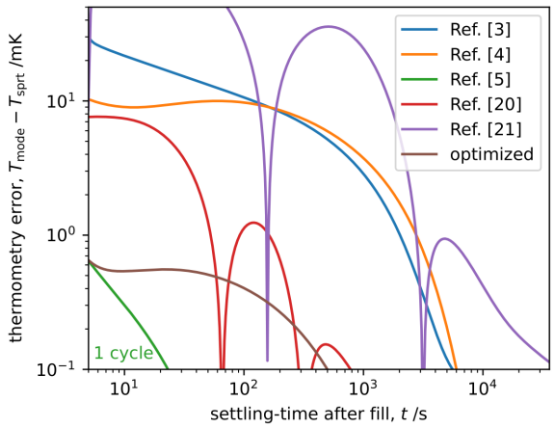

Fig. 7. Meta-analysis of thermal settling-times for several extant optical pressure standards. The thermal load for all cases is the pV-work caused by a 100 kPa fill of argon gas.

Significantly improved performance over Ref. [4] can be achieved with one small design modification: by having the lid of the copper chamber enclose both the thermometer (cSPRT) and the laser beam (cavity mode). A general sketch of how this might look is shown in Fig. 8. The gas volume in the chamber is only 7.5 mL, a factor of 3.4 smaller than Ref. [4]. Simulated performance of this sketched system is labeled as "optimized" in Fig 7. The gradients between the thermometer and the interferometer mode reach 0.1 mK within 500 s, more than an order of

magnitude faster than Ref. [4]. As a comparison of thermal disturbance, the maximum-gradient between the thermometer and interferometer mode is 38 times less than Ref. [4]. Remarkably, the optimized system would enable 3 μPa/Pa accuracy in the optical pressure for sampling times as short as 10 s.

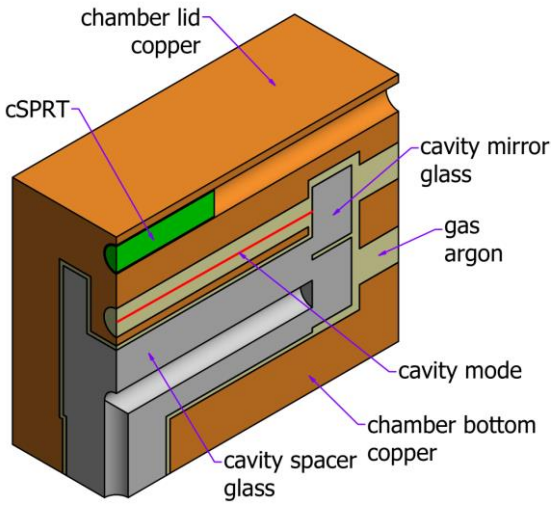

Fig. 8. General sketch of an optimtimized thermal design.

REFERENCES

[1] K. Jousten, J. Hendricks, D. Barker, *et al.*, "Perspectives for a new realization of the pascal by optical methods", Metrologia, vol. 54, 2017, pp. S146-S161.

[2] J. Hendricks, "Quantum for pressure", Nature Physics, vol. 14, 2018, pp. 100.

[3] P. F. Egan, J. A. Stone, J. E. Ricker, J. H. Hendricks, "Comparison measurements of low-pressure between a laser refractometer and ultrasonic manometer", Rev. Sci. Instr., vol. 87, 2016, pp. 053113.

[4] Y. Yang, T. Rubin, J. Sun, "Characterization of a vacuum pressure standard based on optical refractometry using nitrogen developed at NIM", Vacuum, vol. 194, 2021, pp. 110598.

[5] I. Silander, C. Forssén, J. Zakrisson, M. Zelan, O. Axner, "Optical realization of the pascal—Characterization of two gas modulated refractometers", J. Vac. Sci. & Tech. B, vol. 39, 2021, pp. 044201.

[6] Z. Silvestri, D. Bentouati, P. Otal, J. P. Wallerand, "Towards an improved helium-based refractometer for pressure measurements", Acta IMEKO, vol. 9, 2020, issue 5, pp. 305-309.

[7] Y. Takei, K. Arai, H. Yoshida, Y. Bitou, S. Telada, T. Kobata, "Development of an optical pressure measurement system using an external cavity diode laser with a wide tunable frequency range", Measurement, vol. 151, 2020, pp. 107090.

[8] D. I. Babic, S. W. Corzine, "Analytic expressions for the reflection delay, penetration depth, and absorptance of quarter-wave dielectric mirrors", IEEE Journal of Quantum Electronics, vol. 28, 1992, pp. 514-524.

[9] C. Koks, M. P. van Exter, "Microcavity resonance condition, quality factor, and mode volume are determined by different penetration depths", Opt. Express, vol. 29, 2021, pp. 6879-6889.

[10] A. E. Siegman, "Lasers, Ch. 17: Physical Properties of Gaussian Beams", University Science Books, Mill Valley, CA, USA, 1986.

[11] I. Silander, J. Zakrisson, V. S. de Oliveira, C. Forssén, A. Foltynowicz, T. Rubin, M. Zelan, O. Axner, "In situ determination of the penetration depth of mirrors in Fabry-Perot refractometers and its influence on assessment of refractivity and pressure", Opt. Express, vol. 30, 2022, pp. 25891-25906.

[12] M. Durand, Y. Wang, J. Lawall, "Accurate Gouy phase measurement in an astigmatic optical cavity", Applied Physics B, vol. 108, 2012, pp. 749-753.

[13] J. Ricker, K. O. Douglass, J. Hendricks, Sarah White, S. Syssoev, "Determination of distortion corrections for a fixed length optical cavity pressure standard", Measurement: Sensors, vol. 18, 2021, pp. 100286.

[14] Y. Yang, K. Ma, T. Rubin, *et al.*, "Analysis of the outgassing in an optical pressure standard", Proc. of the 6th IMEKO TC16 Conference on Pressure and Vacuum Measurement, 2023, pp. 1-5.

[15] P. F. Egan, J. A. Stone, J. H. Hendricks, J. E. Ricker, G. E. Scace, G. F. Strouse, "Performance of a dual Fabry-Perot cavity refractometer", Opt. Lett., vol. 40, 2015, pp. 3945-3948.

[16] S. Avdiaj, Y. Yang, K. Jousten, T. Rubin, "Note: Diffusion constant and solubility of helium in ULE glass at 23 °C", The Journal of Chemical Physics, vol. 148, 2018, pp. 116101.

[17] https://www.bipm.org/kcdb/comparison?id=80

[18] P. F. Egan, J. A. Stone, J. K. Scherschligt, A. H. Harvey, "Measured relationship between thermodynamic pressure and refractivity for six candidate gases in laser barometry", J. Vac. Sci. & Tech. A, vol. 37, 2019, pp. 031603.

[19] M. Lesiuk, B. Jeziorski, "First-principles calculation of the frequency-dependent dipole polarizability of argon", Physical Review A, vol. 107, 2023, pp. 042805.

[20] P. F. Egan, Y. Yang, "Optical $n(p, T_{90})$ measurement suite: He, Ar, N_2 ", International Journal of Thermophysics, submitted August 2023.

[21] D. Mari, M. Pisani, M. Astrua, M. Zucco, S. Pasqualin, A. Egidi, M. Bertinetti, A. Barbone, "Realisation of an optical pressure standard by a multi-reflection interferometric technique", Measurement, vol. 211, 2023, pp. 112639.